



Research article

Direct methane utilization through benzene dehydroalkylation catalyzed by Co^{2+} sites in ZSM-5 intersections

Martina Aigner^a, Stijn Van Daele^b, Delphine Minoux^b, Nikolai Nesterenko^b, Ruixue Zhao^a, Martin Baumgärtl^a, Rachit Khare^a, Andreas Jentys^a, Christian Schroeder^c, Maricruz Sanchez-Sanchez^{c,**}, Johannes A. Lercher^{a,d,*}

^a Department of Chemistry, Technische Universität München, 85748 Garching, Germany

^b TotalEnergies One Tech Belgium, Zone Industrielle C, Seneffe, 7181, Belgium

^c Institute of Chemical, Environmental and Bioscience Engineering, TU Wien, Getreidemarkt 9/166, 1060 Vienna, Austria

^d Institute for Integrated Catalysis, Pacific Northwest National Laboratory, 902 Battelle Boulevard, Richland, WA 99352, USA



ARTICLE INFO

Keywords:

CH₄ utilization
Ion exchanged zeolites
Benzene alkylation
ZSM-5

ABSTRACT

Cobalt cations exchanged in ZSM-5 are active for the direct dehydromethylation of benzene with CH₄. While toluene is the primary product, an alternate reaction pathway leads also to the formation of biphenyl and phenyltoluene. This not only diminishes the selectivity but also contributes to the deactivation of the catalyst. Temperature-programmed surface reactions show that benzene adsorbs strongly on the exchanged Co^{2+} cations, essentially blocking the sites for alkylation below 400 °C. At temperatures exceeding 400 °C, the partial desorption of benzene enables its reaction with CH₄, leading to the formation of toluene. The formation of biphenyl is kinetically hindered, and its onset is only observed at temperatures above 450 °C. When CH₄ is allowed to chemisorb on Co^{2+} sites prior to exposure to benzene, the formation of toluene is detected at temperatures below 400 °C. By infrared spectroscopy of benzene adsorption and UV–Vis spectroscopic characterization, we identified the existence of intersections in ZSM-5 where three H⁺ are in proximity. The ion exchange of a zeolite lattice Al³⁺ pair in such positions leads to the formation of a Co^{2+} site near a free Brønsted acid site. We observed a correlation between the concentration of this type of Co^{2+} sites and the catalytic activity of Co-ZSM-5 in benzene alkylation with CH₄. This is further supported by the catalytic tests of Co-ZSM-5 materials with specifically a larger proportion of Co sites in sinusoidal channels, as a result of acidic conditions during ion exchange. Based on this, we propose that toluene formation takes place via heterolytic dissociation of CH₄ on a Co^{2+} site at intersections followed by reaction with benzene strongly interacting with an adjacent BAS.

1. Introduction

The tetrahedral symmetry and the strong C–H bonds make methane thermodynamically very stable and relatively unreactive. Activated primarily via steam and CO₂ reforming as well as partial oxidation to synthesis gas, oxyhalogenation is one of the few functionalization reactions that directly converts methane in a single step [1–2].

To convert methane to condensable products, dehydroaromatization with Mo-based catalysts is one of the most explored pathways [3–5]. Elements of group VIII such as Fe, Co and Ni are also known to be suitable catalyst components. Recently, Xu et al., for example, reported Co^{2+} exchanged H-ZSM-5 for the conversion of CH₄ to benzene and

naphthalene [6]. Disadvantages of this process are, however, that temperatures above 600 °C are required and that the catalysts deactivate rapidly by coke formation.

The conversion of CH₄ with benzene to toluene (dehydromethylation) has been suggested as an alternative path to utilize CH₄ for added value products and has been recently reported to occur on zeolite-based catalysts [7–13]. Among the metals and zeolites investigated, Co^{2+} exchanged MFI type zeolites (ZSM-5) appear to be most promising. It has been proposed that the active sites for the CH₄ alkylation of benzene are Co^{2+} cations at the α ion exchange positions of MFI [9,13]. The non-oxidative activation of CH₄ by heterolytic C–H cleavage on strong Lewis acid sites has been tentatively proposed as the catalytic

* Corresponding author at: Department of Chemistry, Technische Universität München, 85748 Garching, Germany.

** Corresponding author at: Institute of Chemical, Environmental and Bioscience Engineering, TU Wien, Getreidemarkt 9/166, 1060 Vienna, Austria.

E-mail address: maricruz.sanchez@tuwien.ac.at (M. Sanchez-Sanchez).

<https://doi.org/10.1016/j.jcat.2024.115686>

Received 6 March 2024; Received in revised form 11 July 2024; Accepted 31 July 2024

Available online 4 August 2024

0021-9517/© 2024 The Authors. Published by Elsevier Inc. This is an open access article under the CC BY-NC-ND license (<http://creativecommons.org/licenses/by-nc-nd/4.0/>).

mechanism [13]. Here, we study the dehydromethylation of benzene with CH₄ on a series of Co-ZSM-5 materials that solely contain exchanged Co²⁺ cations in order to gain mechanistic insights of the reaction as well as identify the effect of location on activity of the catalytic sites.

2. Experimental Section

2.1. Chemicals

High-purity nitrogen (99.999 %), synthetic air (99.995 %), 10 % oxygen in helium (99.995 %), and CH₄ (99.995 %) gases were purchased from Westfalen and used without further purification. Cobalt(II)-acetate (99.99 %) and benzene (anhydrous, 99.8 %) were purchased from Sigma-Aldrich.

2.2. Material synthesis

NH₄-ZSM-5 zeolite (Si/Al = 15, Zeolyst) was calcined in synthetic air (100 mL min⁻¹) for 10 h at 550 °C (10 °C min⁻¹) to obtain the H-form. For preparation of the metal exchanged catalysts, 1 g of H-form zeolite was stirred in 50 mL g⁻¹ Co acetate or Co nitrate solution (2.5 mM – 10 mM) at 80 °C for 15 h. The pH value was adjusted to 6.5 with acetic acid or nitric acid. The resulting suspensions were filtered and washed with water and dried in air.

2.3. Infra-Red spectroscopy measurements

The catalysts were characterized by FTIR measurements with a Nicolet iS50 spectrometer from Thermo Scientific to obtain their acid site concentrations. The spectra were recorded in the range of 4000 – 650 cm⁻¹ on thin catalyst pellets. After heating to 450 °C for 1 h under vacuum (10 °C min⁻¹, 10⁻⁷ mbar), pyridine (0.5 mbar) was adsorbed at 150 °C for 1 h. To obtain only chemisorbed pyridine the sample was under vacuum (10⁻⁷ mbar) for one hour. With this, we have quantified the concentration of Brønsted acid sites (BAS) in the parent sample H-ZSM-5 and in the Co-ZSM-5 catalysts (see SI section S1 for details).

Benzene adsorption measurements were carried out in a Bruker ifs 66v/S FTIR spectrometer. The spectra were recorded in the range of 4000 – 650 cm⁻¹ on thin catalyst pellets. After heating to 450 °C for 1 h under vacuum (10 °C min⁻¹, 10⁻⁷ mbar), benzene was adsorbed stepwise from 7.0 • 10⁻³ – 11 mbar. For analysis, the SiOHAl band at 3610 cm⁻¹ and the C–C band at 1478 cm⁻¹ were used for BAS coverage and benzene uptake, respectively.

2.4. Atomic absorption spectroscopy

For investigation of the element contents in the prepared catalysts graphite-tube atomic absorption spectroscopy (GT-AAS) was performed on a Solaar M5 AA-Spectrometer from ThermoFischer.

2.5. Catalytic testing

The activity of the catalysts was tested in a 1/4" quartz glass plug flow reactor between 500 and 560 °C, under atmospheric pressure. The catalysts were activated in a mixture of 10 % oxygen in helium at 550 °C (10 °C min⁻¹) for 2 h. Before starting the reaction, the reactor was purged with nitrogen. The reaction was conducted in nitrogen atmosphere with varied ratios of CH₄/benzene = 33 – 170, and WHSV=0.2 – 2.2 h⁻¹. Reactants and products were analyzed by a GC System Agilent 7890B or a mass spectrometer Omnistar® by Pfeiffer Vacuum.

2.6. Temperature programmed surface reaction

For TPSR, the catalyst was activated in a 1/4" quartz glass plug flow reactor at 550 °C in a mixture of 10 % oxygen in helium (atm). After

purging with inert for 1 h, the catalyst was exposed to CH₄ or benzene at 200 °C for 2.5 h and 0.5 h, respectively. After purging with inert, the catalyst was heated up to 550 °C (5 °C min⁻¹) in benzene (5 mbar) or CH₄ (750 mbar). Reactants and products were analyzed by a mass spectrometer Omnistar® by Pfeiffer Vacuum.

3. Results and discussion

3.1. Synthesis of Co-ZSM-5 with ion exchanged Co²⁺ as the only Co species

A series of Co-ZSM-5 catalysts with different Co²⁺ loadings were prepared by ion exchange of a parent H-ZSM-5 (Si/Al = 15), following a protocol that minimizes the formation of CoO_x particles (see SI section 1 and Experimental). Other methods that introduce larger concentrations of Co²⁺ cations, such as impregnation, have been shown to form CoO_x particles (Figure S1 in SI). The degree of ion-exchange in Co-ZSM-5 was evaluated by pyridine adsorption, determining the concentration of remaining Brønsted acid sites (BAS) in H-ZSM-5 after Co exchange (Table S1 in SI). The concentration of BAS exchanged with Co²⁺ cations was calculated considering that after a treatment in acetic acid solution, equivalent to the ion exchange procedure, 780 μmol g⁻¹ of BAS were available for ion-exchange. For catalysts with Co contents lower than 170 μmol g⁻¹ the ratio of exchanged BAS per Co²⁺ was 2.0 ± 0.1. With increasing Co loading, this BAS/Co ratio decreased slightly, but remained ≥ 1.7 ± 0.1. This is consistent with a majority of divalent Co²⁺ ions exchanging at proximate Al tetrahedra, thus, one Co²⁺ replaced two BAS. The concentration of Al pairs in this H-ZSM-5 is 40 %, measured by Co²⁺ ion exchange following the protocol of Dedecek et al. [14].

3.2. Activity of Co²⁺ sites in Co-ZSM-5 catalysts for the alkylation of benzene with CH₄

The reaction of CH₄ and benzene was performed at 550 °C and under a large excess of CH₄, in order to increase the thermodynamic limit of benzene conversion [8]. The partial pressure ratio of CH₄ to benzene in our catalytic tests was 80 unless else is stated. First, we tested the activity of H-ZSM-5 in benzene alkylation with CH₄ and did not observe products, indicating that BAS in H-ZSM-5 are not active for this reaction under the conditions explored here. Therefore, the activity of Co-ZSM-5 catalysts is compared based on benzene consumption rates obtained at differential conditions and normalized per Co atoms present in the sample. In Fig. 1, Co-based turnover frequencies (TOF_{Co}) are correlated to the concentration of Co²⁺ in each Co-ZSM-5. A similar trend is obtained if the TOF_{Co} is calculated for toluene rates of formation (Figure S2), because the selectivity to toluene for all tested samples is in the range 80–95 %.

When examining the activity expressed as TOF_{Co}, Co-ZSM-5 catalysts can be grouped into two categories depending on the Co²⁺ loading (Fig. 1). An average TOF_{Co} of 3.5 • 10⁻⁵ s⁻¹ (dashed line in Fig. 1) was observed for samples with low loadings of Co²⁺. Conversely, the TOF_{Co} increased with the concentration of Co²⁺ exchanged in ZSM-5, for samples prepared at Co loadings above ca. 150 μmol g⁻¹. At the ion exchange upper limit of 333 μmol g⁻¹, the TOF_{Co} was approximately one order of magnitude higher than the TOF at low Co²⁺ exchange degrees.

The specific activity of Co increased with Co loading, as shown in Fig. 1. This is attributed to the formation of two types of Co²⁺ sites, one less active at low loadings and one more active at high ion exchange loadings. Origins for this different activity may stem from the structure (nuclearity) of the Co²⁺ sites or from their specific location at exchange sites, i.e., from the geometry and environment provided by the zeolite framework. We have determined the ratio of BAS exchanged per Co²⁺ by IR spectra of adsorbed to be ≥ 1.8 for Co-ZSM-5 with Co loadings up to ca. 300 μmol g⁻¹ (Table S1). This indicates that the dominant Co²⁺ species are single Co²⁺ cations exchanged at paired Al T-sites. We attribute the slight decrease in BAS/Co ratio at high Co loadings to the

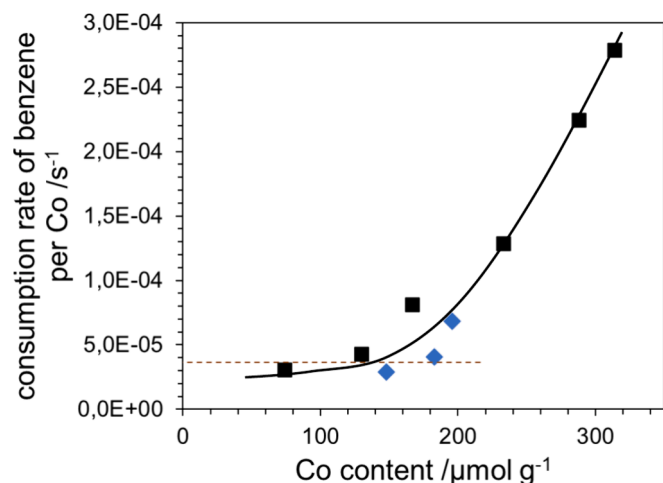


Fig. 1. Activity of Co-ZSM-5 materials with different loadings, shown as consumption rate of mols of benzene per mol Co. Results for H-ZSM-5 ion exchanged with Co acetate (black square) are compared to materials prepared by ion exchange of Co nitrate (blue diamonds). $T=550\text{ }^{\circ}\text{C}$, 1 atm, 400 mbar CH_4 , 5 mbar benzene, $\text{WHSV}=0.6\text{ h}^{-1}$ (conversion range 0.2–3.6 %). (For interpretation of the references to color in this figure legend, the reader is referred to the web version of this article.)

formation of a small fraction of other species with a nominal BAS/Co exchange ratio of one, e.g., $[\text{CoOH}]^+$ exchanged on a single Al site or $[\text{Co-O-Co}]^{2+}$ structure exchanged on Al pairs [14]. The presence of Co oxide nanoparticles was not observed by TEM (see Figure S1 in SI) and can be ruled out based on the charge balance of the exchanged sites (Table S1 in SI).

Several spectroscopic techniques were applied to confirm the homogeneity of Co^{2+} ions in the series of Co-ZSM-5 samples. Co K-edge in-situ X-ray absorption (see Figures S7 and S8) showed that the majority of Co exists as Co^{2+} in the studied Co-ZSM-5 materials. The EXAFS spectra for samples with 230–330 $\mu\text{mol}_{\text{Co}}\text{ g}_{\text{cat}}^{-1}$ shows a contribution of Co-Co scattering (coordination number ca. 0.65, Table S4), indicating the possible presence of Co species other than bare Co^{2+} exchanged ions at these Co loadings. On the other hand, IR spectra of adsorbed CO showed the presence of only isolated Co^{2+} sites for samples with Co loading up to 314 $\mu\text{mol}_{\text{Co}}\text{ g}_{\text{cat}}^{-1}$ (Figure S6). For samples with Co loadings above this value, there is evidence of a small fraction of $[\text{Co-O-Co}]^{2+}$ species being reduced in presence of CO (see SI Section 6 for details).

Overall, for samples with $\text{BAS}/\text{Co} \geq 1.8$, we assume that the fraction of multinuclear Co species is negligible. Additionally, it is important to highlight that considering the subpar catalytic performance of Co-ZSM-5 samples containing CoO_x nanoparticles (Fig. S2A) and the documented lower activity of Zn-O-Zn in CH_4 activation compared to Zn^{2+} isolated ions, [15] the presence of small concentrations of CoO_x and Co-O-Co species is not expected to make a significant contribution to the reaction rates. Based on this, the discussion of activity-structure relationships here is limited to Co-ZSM-5 catalysts with Co loadings below 315 $\mu\text{mol}_{\text{Co}}\text{ g}_{\text{cat}}^{-1}$.

As for the location of Co^{2+} sites in ZSM-5, it is well-established that the pH of the ion exchange solution plays a significant role in determining the extent of exchange and the specific location of metal ion species [16–17]. Therefore, in order to investigate further the role of location of Co^{2+} sites for their intrinsic activity, we have prepared several Co-ZSM-5 samples via ion exchange with Co(II) nitrate, which provides an exchange medium more acidic than Co(II) acetate. The activity of Co-ZSM-5 prepared with Co nitrate is also shown in Fig. 1, and, interestingly, the observed TOF_{Co} are significantly different from the expected in the acetate series, at least in the range 150–180 $\mu\text{mol g}^{-1}$. At differential conversions (1.5–2.5 %, Figure S3), the selectivities to products are similar for all ion-exchanged Co-ZSM-5. However, it is

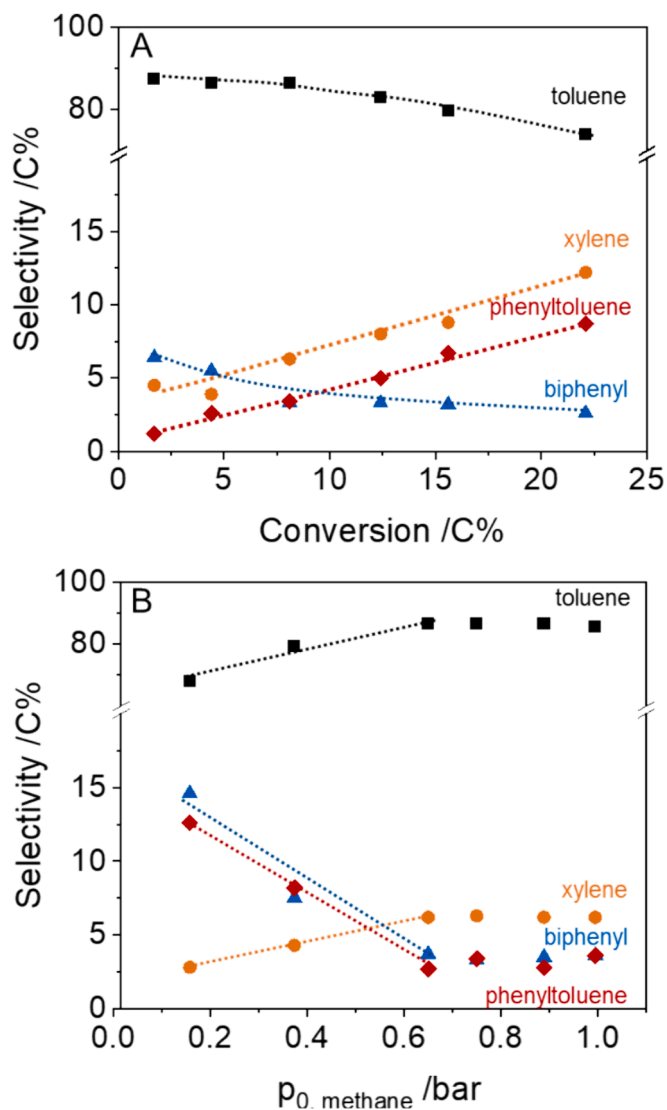


Fig. 2. Selectivity towards products in the CH_4 alkylation of benzene over Co-ZSM-5 catalyst (314 $\mu\text{mol}_{\text{Co}}\text{ g}^{-1}$). C_7 (toluene, square), C_8 (xylenes, circle), C_{12} (biphenyl, triangle) and C_{13} (phenyltoluene, diamond) as a function of A) the conversion of benzene, and B) the partial pressure of CH_4 . $T=550\text{ }^{\circ}\text{C}$, 1 atm, $p_{\text{benzene}}=5\text{ mbar}$, p_{CH_4} 10–960 mbar (750 mbar in A), $\text{WHSV}=0.1\text{--}2.5\text{ h}^{-1}$.

worth mentioning a slight increase of xylenes at expense of toluene for nitrate-exchanged materials.

To comprehend the underlying reasons behind the varying TOF_{Co} observed in Fig. 1 across a range of Co-ZSM-5 catalysts containing solely Co^{2+} exchanged ions, we will begin by examining the fundamental processes involved in the activation of methane and benzene on Co-ZSM-5.

3.3. Reaction pathways of benzene alkylation with CH_4 over Co-ZSM-5

In the first step, we investigate the activity and product distribution of a typical Co-ZSM-5, varying concentrations of benzene, toluene and CH_4 in the feed (Table 1). For benzene dehydroalkylation with CH_4 (Entry 1) toluene and H_2 were the main product, but also xylenes, phenyltoluene and biphenyl were formed. The evolution of selectivity with conversion (Fig. 2A) shows that toluene and biphenyl are primary products of benzene, while xylenes and phenyltoluene are secondary products. If only benzene was passed over the catalyst, the activity was five times lower and the only product was biphenyl (Entry 2). However, a feed of pure toluene (Entry 3) led to xylenes together with small

Table 1

Formation rates of CH₄, benzene, toluene, xylenes, biphenyl and phenyltoluene with different feed compositions over Co-ZSM-5 with 314 μmol/g Co loading. T=550 °C, 1 atm, p_{0, CH₄} = 400 mbar, WHSV=0.6 h⁻¹.

Entry	Reactants	P _{aromatics} in the feed /mbar	Conversion Benzene /Toluene / %	Formation rate CH ₄ / mol s ⁻¹ g ⁻¹	Formation rate toluene / benzene / mol s ⁻¹ g ⁻¹	Formation rate C _{8/9} / mol s ⁻¹ g ⁻¹	Formation rate C ₁₂ / mol s ⁻¹ g ⁻¹	Formation rate C ₁₃ / mol s ⁻¹ g ⁻¹
1	Benzene + CH ₄	5.1	3.7	–	4.9·10 ⁻⁸	0.2·10 ⁻⁸	1.1·10 ⁻⁸	0.9·10 ⁻⁸
2	Benzene	5.1	0.7	–	–	–	1.4·10 ⁻⁸	–
3	toluene	4.9	12.4	5.1·10 ⁻⁹	6.6·10 ⁻⁸	3.2·10 ⁻⁸	–	2.5·10 ⁻⁹
4	Benzene + toluene	2.5 / 2.5	– / 31.7	3.8 ·10 ⁻⁹	–	3.2·10 ⁻⁸	6.1·10 ⁻¹⁰	3.3·10 ⁻⁸
5	Toluene + CH ₄	5.1	14.1	–	6.1·10 ⁻⁸	5.3·10 ⁻⁸	–	1.1·10 ⁻⁹
6	CH ₄	0	/	/	6,2·10 ⁻¹⁰ / 2.1·10 ⁻⁹	5.4·10 ⁻¹⁰	–	–

fractions of benzene, CH₄ and phenyltoluene; biphenyl was not detected.

The formation of xylenes and benzene is attributed to toluene disproportionation. Moreover, the formation of phenyltoluene, while absent as a product from the pure benzene stream, suggests that this product stems from the reaction of toluene with benzene and not from methylation of biphenyl.

Consistently, it was observed that when benzene and toluene were co-fed (in absence of CH₄) the highest rates in the formation of phenyltoluene were achieved (Entry 4, 3.3·10⁻⁸ mol s⁻¹ g⁻¹). In comparison, the biphenyl yield was significantly lower than during the conversion of benzene. This is attributed to the lower partial pressure of benzene in the feed of this experiment. The decrease in the rate of biphenyl formation was almost two orders of magnitude, suggesting that toluene is significantly more reactive than benzene. Co-feeding toluene and CH₄ (Entry 5) mainly led to xylenes. Finally, when feeding only CH₄ on Co-ZSM-5, benzene was formed with low rates via methane dehydroaromatization [6].

Based on these experiments, we propose a reaction network for CH₄ and benzene as shown in Scheme 1. Two main pathways are involved, i. e., (i) the CH₄ dehydroalkylation of benzene to toluene, and subsequently to xylenes and a small fraction of C₉₋₁₁ and (ii) the bimolecular reaction of benzene to produce biphenyl. A fraction of toluene formed via pathway (i) reacts with benzene to produce phenyltoluene (iii). Finally, the contribution of toluene disproportionation to the formation of xylenes (iv) has to be considered at conversions above 10 %, as the reactivity of toluene is one order of magnitude higher than that of benzene (Table 1, Entries 1 and 4 and Entries 2 and 3).

Fig. 2B shows selectivities to products of Co-ZSM-5 when tested at 550 °C and different CH₄ pressures, measured at conversions in the

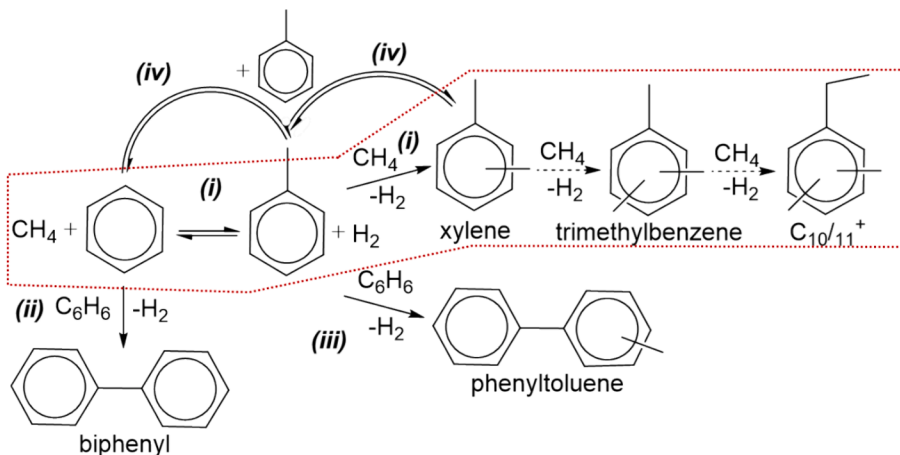
range 5–8 %. In accordance with the reaction pathways depicted in Scheme 1, the alkylation products toluene and xylenes increased with CH₄ partial pressure. Conversely, the selectivity towards the direct product of benzene reaction (biphenyl) decreased.

3.4. Surface mechanism of benzene dehydroalkylation with CH₄

Next, the surface reactions of activated methane and benzene were studied by temperature programmed surface reactions (TPSR) (Fig. 3 and Section S5 in SI). When CH₄ was preadsorbed at 200 °C and a stream of benzene was passed over the catalyst, formation of toluene started at 200 °C and was nearly complete at 450 °C showing a pronounced maximum at 350 °C. Conversely, when benzene was pre-adsorbed and flowing CH₄ was passed over the catalyst, neither toluene nor biphenyl were formed below 350 °C. The onset of toluene formation is observed at 350 °C, and biphenyl formation is only observed above 450 °C. On the other hand, we observe benzene desorption predominantly at temperatures above 300 °C, and this process is completed at 450–500 °C.

These results suggest that the same catalytic sites used for CH₄ activation are also sites where benzene strongly adsorbs. Therefore, only when strongly adsorbed benzene desorbs from at least a fraction of active sites at T>350 °C is the formation of toluene possible. TPSR also shows that the formation of biphenyl (and subsequent products such as C₁₃) is kinetically hindered below 450 °C, suggesting that this reaction possesses a higher energy of activation compared to benzene dehydroalkylation with CH₄. We did not detect any formation of H₂ in absence of benzene (Fig. 3B1, dashed line) and therefore we conclude that the catalyst does not dehydrogenate CH₄.

Finally, we observed neither the desorption of chemisorbed CH₄ nor



Scheme 1. Reaction network of benzene with CH₄ over Co-ZSM-5, with pathways (i) dehydroalkylation of benzene and subsequent products with CH₄; ii) biphenyl formation; iii) phenyltoluene formation; iv) toluene disproportionation.

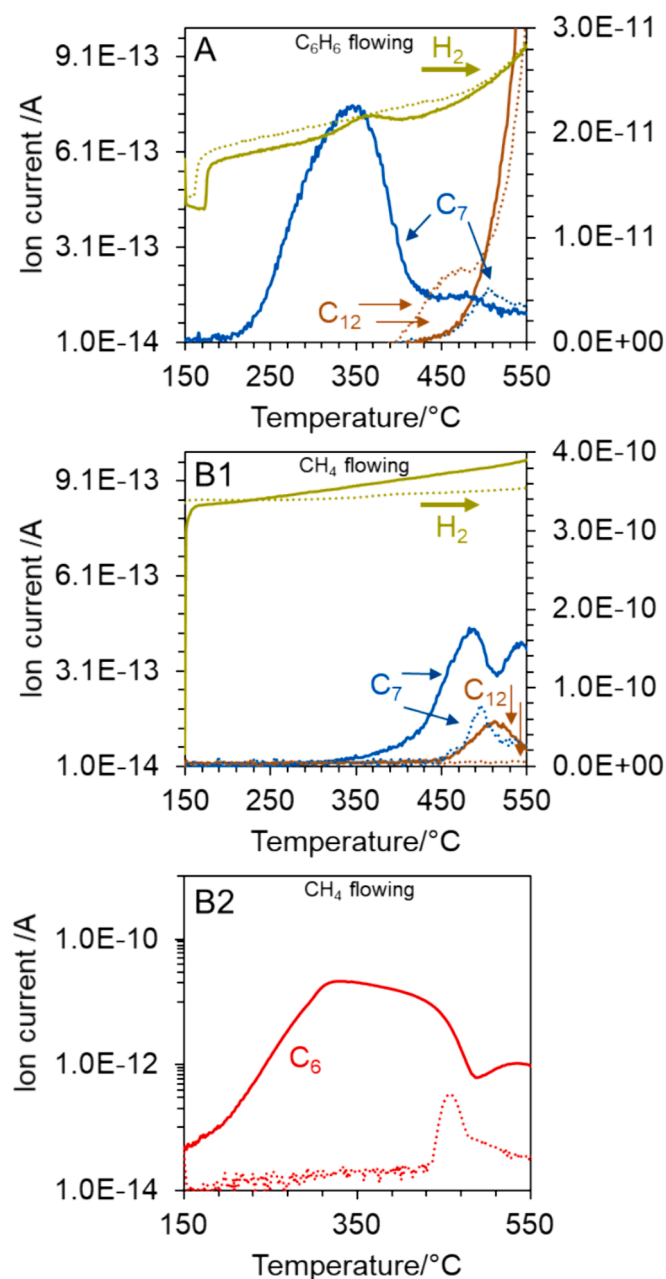


Fig. 3. Temperature programmed reaction over Co-ZSM-5 with $314 \mu\text{mol}_{\text{Co}} \text{g}^{-1}$ of A) benzene (5 mbar) after the catalyst was exposed to CH_4 (200 °C, 750 mbar, 2.5 h), and B1) CH_4 (750 mbar) after the catalyst was exposed to benzene (200 °C, 5 mbar, 0.5 h) with 5°C min^{-1} . In B2 it is shown the signal of benzene in corresponding to experiment B1. The y-axis represents the ion current measured by mass spectroscopy: toluene (C_7 , blue), benzene (C_6 , red), and biphenyl (C_{12} , brown) left, and hydrogen (green) on the right axis. Blank experiments in which the TPRs were performed on a clean Co-ZSM-5 without pre-exposure to any reactant are shown in dotted lines. (For interpretation of the references to color in this figure legend, the reader is referred to the web version of this article.)

the formation of oxidation products or any oxidation products when steam was passed over the surface bound methane at 135 °C (see details in Section 5 SI). This indicates that methane does not form methoxy species on Co-ZSM-5.

Considering all these experimental observations, our hypothesis is that CH_4 adsorbs dissociatively on Co^{2+} sites either by forming a CH_3^- bound to Co^{2+} and H^+ to an adjacent oxygen – analogous to what has been reported for Zn^{2+} strong Lewis acid sites [15,18] and recently also

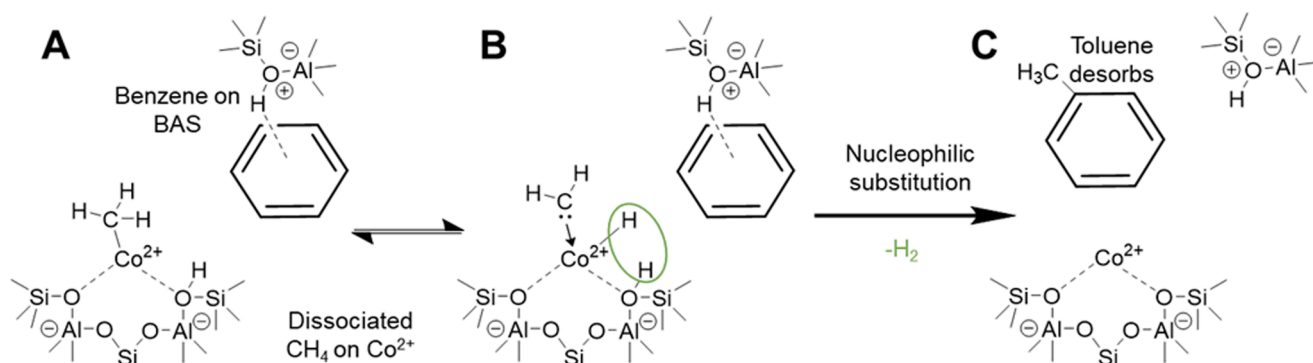
for Co^{2+} in zeolites [6] – or, alternatively, by oxidatively adsorbing onto adjacent Co^{2+} sites, forming a hydride on the second Co^{2+} that could subsequently activate benzene [19–20]. However, the latter mechanism implies that the reaction kinetics show a first-order dependency with benzene pressure. The experimentally obtained reaction orders in benzene are all positive but well under 0.5 (see SI, Table S2). Hence, our proposition is that CH_4 undergoes heterolytic dissociation facilitated by Co^{2+} sites, as depicted in Scheme 2, and the $\text{CH}_3\text{-Co}^{2+}$ structure leads to the formation of a CH_2 carbene adduct and a hydride [21]. The subsequent reaction of the carbene with benzene via nucleophilic substitution – together with formation of H_2 – is facilitated by the stabilization of benzene in an adjacent BAS (Scheme 2, left).

3.5. On the location of Co^{2+} sites in MFI framework and its effect on activity

A possible explanation of the TOF_{Co} increase with Co^{2+} loading depicted in Fig. 1 is the formation of highly active sites in Co-ZSM-5 related to particular ion exchange positions becoming occupied at high loadings. To identify whether such highly active sites exist, we next investigate the location and type of Co^{2+} species in this series of Co-ZSM-5. Using UV–vis spectroscopy we derived a tentative map of the location of Co^{2+} ions in the ZSM-5 framework [13–14,21–23]. In literature, the activity in benzene alkylation with CH_4 has been attributed to Co^{2+} in α positions [9,13]. Fig. 4A shows the concentrations of Co^{2+} in α , β and γ positions, exchanged on Al pairs, based on band assignments in the literature, [14] as derived from spectra in Figures S9 and S10. Notably, the UV–vis band attributed to α position is only visible for samples with Co loadings of $180 \mu\text{mol}_{\text{Co}} \text{g}_{\text{cat}}^{-1}$ or higher. In all cases, only a small proportion of Co is absorbing in the region of 15000 cm^{-1} , assigned to α sites. It should be noted that recent studies detect an increase in the UV–vis absorption in this region for samples with Co oxide-like species [21]. The small intensity of the absorption band at 15000 cm^{-1} in this Co-ZSM-5 series is in good agreement with our spectroscopic results, which showed negligible concentrations of oxide-like species. In addition, the absence of absorption bands in the region $29000\text{--}30000 \text{ cm}^{-1}$ (Figure S11 in SI) indicates that Co^{3+} species are not formed, [21] confirming the absence of Co_3O_4 oxide-like species in the studied Co-ZSM-5 catalysts. The concentrations of Co exchanged in β and γ positions increase monotonically with Co loading in the whole range studied. Interestingly, for samples prepared by ion exchange with Co nitrate, a larger fraction of Co^{2+} is exchanged in γ positions. The differences in siting can be attributed to the different pH of the ion exchange solution species [16–17].

Infrared spectra of benzene were used to obtain additional information on the location of BAS before and after introducing Co in ZSM-5, which indirectly reveals the positions of ion exchanged Co^{2+} . Two main features are monitored upon benzene adsorption, i.e., the appearance of an absorption band at 1472 cm^{-1} and the decrease of the absorption band at 3610 cm^{-1} (Figures S12 and S13). The band at 1472 cm^{-1} is attributed to benzene adsorbed on Co^{2+} , using the similarity to a band at 1468 cm^{-1} identified to be caused by benzene interacting with Cu^{2+} in ZSM-5 [24]. The slight blue shift with respect to Cu^{2+} ions is consistent with the strong Lewis acid character of Co^{2+} species, leading to a weaker C–C bond of benzene upon adsorption than when interacting with Cu^{2+} . The concentration of BAS interacting with benzene is calculated via the decrease of intensity of the SiOHAl band at 3610 cm^{-1} (and the increase of the C–C vibration at $\sim 1475 \text{ cm}^{-1}$) following analysis method by Baumgärtl et al [25].

For the parent H-ZSM-5 washed with acetate solution (blank experiment), the decrease of the BAS O–H vibration with increase of benzene uptake follows a linear correlation at low benzene pressures (Fig. 5), with a slope of ~ 3.0 . This indicates that three BAS are interacting with one benzene molecule. We speculate that these sites are located at the channel intersections. In this position, one benzene molecule can perturb the O–H vibration of up to three protons that are in proximity,



Scheme 2. Proposed mechanism of dehydroalkylation of benzene with CH₄ in Co-ZSM-5. A) CH₄ dissociated on Co²⁺ with benzene adsorbed on a nearby Brønsted acid site. B) Formation of a resonant hydride-carbene complex on Co²⁺ sites. This hydride and the proton in adjacent O form H₂, leaving the CH₂ carbene adduct. C) Nucleophilic substitution of carbene on the adjacent benzene leads to formation of toluene, restoring BAS and Co²⁺ site.

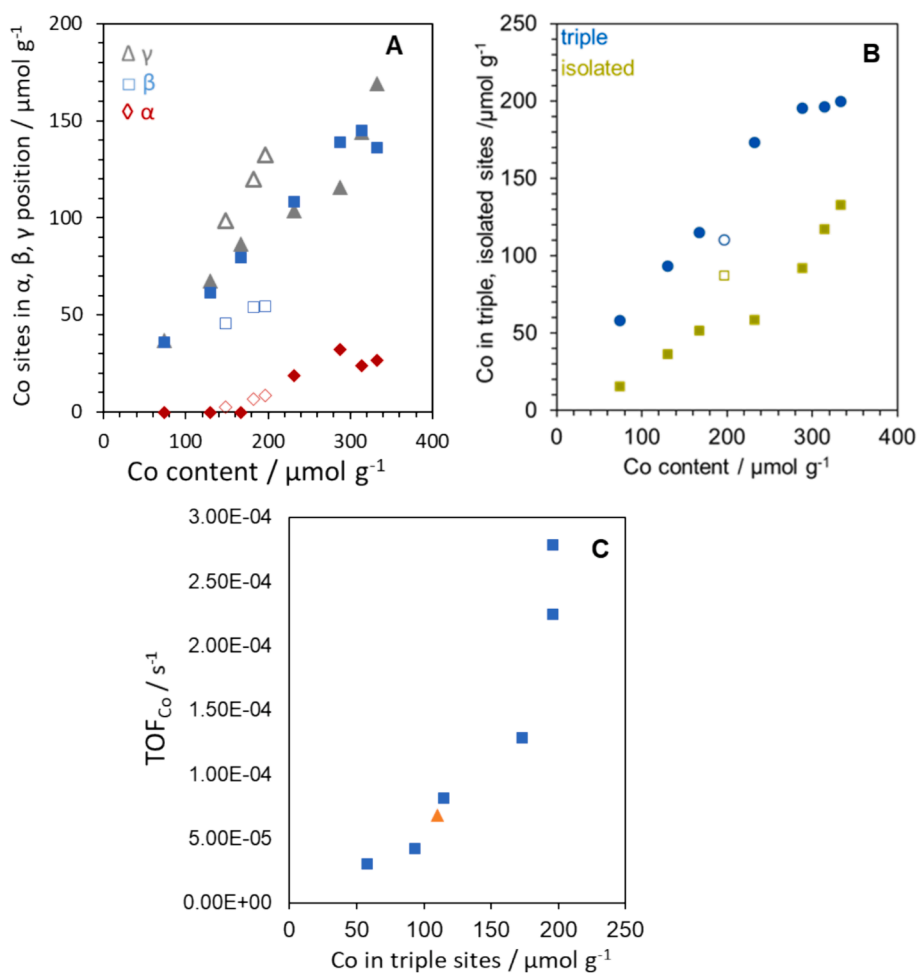


Fig. 4. A) Concentration of Co exchanged in α , β and γ position from UV-Vis deconvolution. B) Concentration of Co exchanged in triple or isolated sites, according to benzene adsorption IR. Full symbols for Co-ZSM-5 prepared with Co(II) acetate, hollow symbols for Co-ZSM-5 prepared with Co(II) nitrate. C) TOF_{Co} as benzene consumption per total Co content vs Co in triple sites as quantified by benzene adsorption IR. Hollow symbols in A) and B), and orange triangles in C) indicate Co-ZSM-5 prepared with Co(II) nitrate. Reaction conditions as in Fig. 1. (For interpretation of the references to color in this figure legend, the reader is referred to the web version of this article.)

shifting the O-H IR absorption to lower wavenumbers. The presence of multiple sets of 3 BAS close enough to interact with one molecule of benzene indicates that the proximity between Al sites in the framework is higher than expected from the statistical distribution of Al in a ZSM-5 with Si/Al ratio of 15. This is not surprising given the uneven distribution of Al across zeolite crystals as reported in literature [26–27].

On Co-ZSM-5 materials, the OH vibration of BAS is not significantly affected at low benzene uptakes, pointing to a preferential adsorption of benzene on Co²⁺ sites. Once the benzene uptake is sufficiently increased, we observe a linear decrease in the BAS O-H band with slopes ranging from 1 to 3 depending on the Co loading (Fig. 5A and S14). On one hand, a slope or ratio of 1:1 is expected when benzene adsorbs on mostly

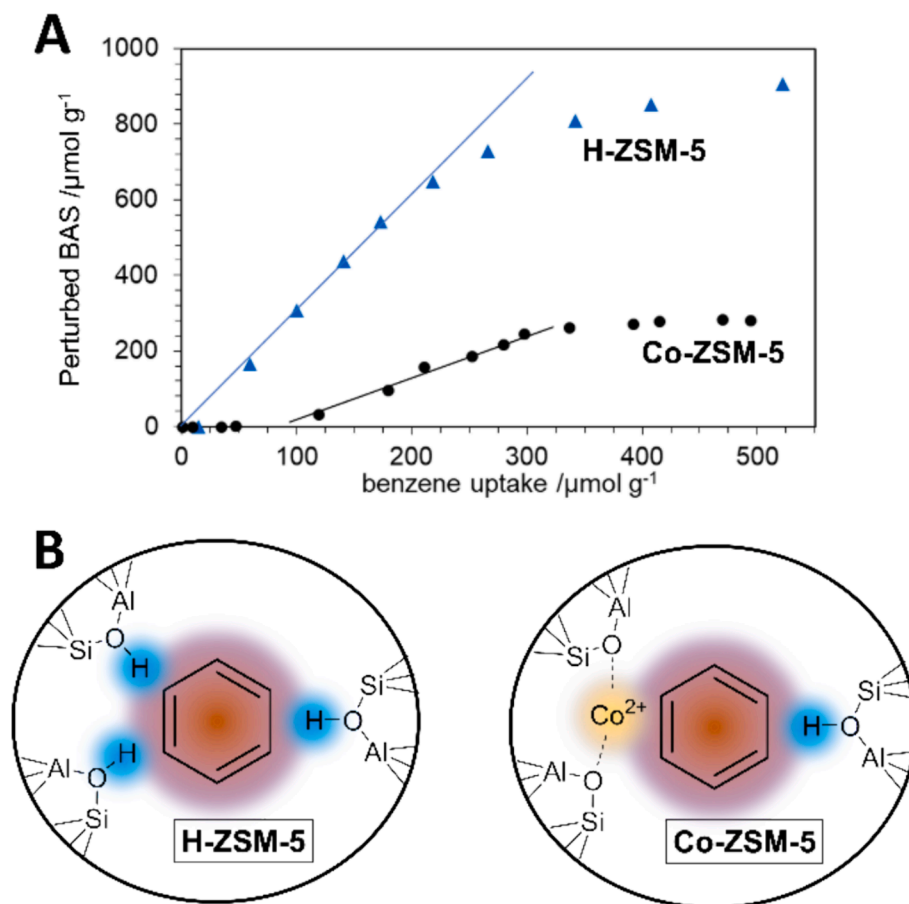


Fig. 5. A) Benzene adsorption on H-ZSM-5 (blue triangle), and Co-ZSM-5 with $314 \mu\text{mol Co g}^{-1}$ (black circle). Activation for 1 h, $400 \text{ }^\circ\text{C}$ at $p < 10^{-7}$ mbar. $p_{0,\text{benzene}} = 7.0 \cdot 10^{-3} - 1.1 \cdot 10^1$ mbar, $T=100 \text{ }^\circ\text{C}$. The linear region shows BAS:benzene ratios near 3 (H-ZSM-5) and 1 (Co-ZSM-5). B) Schematic representation of a “triple site” where three protons are located in an intersection of the MFI framework, and the outcome of exchanging Co^{2+} to two paired Al sites. The change in perturbed BAS/benzene ratio allows us to calculate the proportion of Co exchanged in intersections (Section S7). (For interpretation of the references to color in this figure legend, the reader is referred to the web version of this article.)

isolated BAS. Additionally, the adsorption of benzene in Co-sites can also perturb the O–H band of one neighboring BAS, shifting the IR absorption of this bond to much lower wavenumbers and therefore causing a decrease of the characteristic SiOHAl band. This will be expected to occur when Co has exchanged protons in Al pairs that are part of a triple site (Fig. 5B), leading to a perturbed BAS:benzene ratio of 1. Therefore, upon exchange of increasing concentrations of Co^{2+} on triple sites, the interaction of benzene with BAS gradually changes from a 1:3 ratio to a 1:1 ratio (Figure S14).

By comparison with the benzene adsorption on the parent H-ZSM-5, we derive the concentration of Co that has been exchanged in “triple sites” (those for which one molecule of benzene can simultaneously interact with 3 protons) and, by difference, the concentration of Co^{2+} exchanged in “isolated sites” (that is, positions where one benzene molecule cannot interact with more than one BAS). The details of this quantification are summarized in Section 7 of SI, and the results are shown in Fig. 4B. It can be seen that the Co^{2+} ion exchange occurs both in triple and non-triple sites, and the concentration on both sites increases with loading. It should be noted that for samples prepared using Co(II) nitrate, the exchange in the intersections (“triple sites”) is less favored in comparison to samples prepared with Co(II) acetate. This confirms the different siting detected by UV–vis spectroscopy for samples prepared under more acidic ion exchange, and supports a correlation between Co in triple sites with the Co in β position, and between the Co ions in isolated sites with more constrained γ positions.

Based on the kinetic results with Co-ZSM-5, we conclude that the active sites for dehydroalkylation of benzene with CH_4 are bare Co^{2+}

ions exchanged in MFI. The activity of Co-ZSM-5 in dehydroalkylation of benzene with CH_4 has been previously attributed to such Co^{2+} in α positions [9,28]. The present data do not support this attribution. We have measured a TOF_{Co} of ca. $3.5 \cdot 10^{-5} \text{ s}^{-1}$ (based on benzene consumption rate) for materials in the absence of α sites, demonstrating that exchanged Co^{2+} ions in other positions are equally active. The increase of TOF with Co loading in the range 180 to $300 \mu\text{mol g}^{-1}$ observed in Fig. 1 could be attributed in a first attempt to the contribution of highly active Co in α positions. However, a Co-ZSM-5 prepared with nitrate precursor and containing $196 \mu\text{mol g}^{-1}$ of Co shows low activity (compatible with a TOF_{Co} of $3.5 \cdot 10^{-5} \text{ s}^{-1}$) in spite of a measurable concentration of α sites. Conversely, a Co-ZSM-5 containing $167 \mu\text{mol g}^{-1}$ and prepared via acetate exchange is twice as active (TOF_{Co} of $8.1 \cdot 10^{-5} \text{ s}^{-1}$), in spite of not containing any Co in α positions. Therefore, we conclude that the increase in TOF with Co loading is not due to the formation of highly active sites in α positions (Figure S15). On the contrary, in Fig. 4C it can be seen that Co-normalized activity and its increase with Co loading correlates to the concentration of Co^{2+} that was exchanged in “triple sites” resulting in a Co^{2+} site near a BAS (Fig. 5B).

The increase in the TOF_{Co} observed for Co-ZSM-5 with Co loadings above $180 \mu\text{mol g}^{-1}$ is not related to the energy barrier, because a consistent apparent energy of activation of 122–126 kJ/mol was measured for catalysts with significantly different Co loadings (Table S2 and Figure S4). For Zn-exchanged ZSM-5, the position of Zn^{2+} ions was found to affect their intrinsic activity in CH_4 conversion [18,29–30]. Notably, Nozik et al. reported on a series of Zn-ZSM-5 catalysts, where the majority of Zn existed as bare Zn^{2+} ions, and observed an increase in

propane dehydrogenation rates with Zn loading [31]. They attributed this effect to the localization of Zn^{2+} cations either at increasingly distant pairs of Al atoms or at the β -site (intersections) in the MFI framework. The location of sites in MFI intersections is often connected to catalytic advantages linked to entropic effects [32]. In our case, the bimolecular nature of the reaction might be sufficient to require a less constrained environment. Additionally, the presence of Brønsted acid sites sufficiently close to interact simultaneously with a benzene molecule indicates the potential to generate a Co-BAS pair upon exchange (Fig. 5B), which is suitable to catalyze the reaction via the mechanism proposed in Scheme 2.

Finally, when comparing the rates for Co^{2+} sites with identical nature and location (Fig. 4C), the upward trend of TOF vs. Co^{2+} loading remains prominent. Consequently, we conclude that the geometry of the specific ion exchange site plays a key role in the stabilization of highly active vs. less active Co^{2+} sites. Therefore, for the Co-ZSM-5 materials presented here, in the absence of Co species other than bare Co^{2+} exchanged sites and with the active sites located in the MFI intersections, those Al pairs that can stabilize more symmetric Co^{2+} will be exchanged first, leading to less active species. In contrast, Al distant pairs will be only exchanged at high Co loadings, but these will result in distorted geometries of the exchanged ions and, hence, higher catalytic activity in CH_4 dissociation, analogous to Zn-ZSM-5 [29–30].

4. Conclusions

Benzene undergoes methylation with CH_4 on Co-ZSM-5 in which a majority of Co^{2+} was exchanged as bare Co^{2+} ions on Al pairs. Two main reaction pathways have been identified, i.e., the dehydroalkylation of benzene with methane to form toluene, and the dehydrogenative dimerization of benzene to form biphenyl. Despite the substantial biphenyl formation with Co-ZSM-5 in absence of methane, the lower energy barrier for toluene formation tends to favor dehydroalkylation.

Based on our TPSR experiments, we conclude that Co^{2+} sites exchanged in Al pairs activate both CH_4 and benzene. Benzene strongly adsorbs in these sites, poisoning them for any further activation of CH_4 until the temperature of desorption has been reached (>350 °C). The activity per Co^{2+} site in benzene hydroalkylation with CH_4 increases with higher concentrations of Co exchanged in the zeolite. This effect is especially pronounced for Co^{2+} sites at the MFI intersections where three protons were in proximity in the parent H-ZSM-5. These sites form upon exchange an active Co^{2+} – BAS pair that allows for the activation of CH_4 on Co^{2+} sites and stabilization of benzene on the BAS. This facilitates the nucleophilic substitution of benzene by carbene to form toluene. This mechanistic proposal explains quantitatively why an activity correlation is found with β -sites at the intersections of the MFI framework and not with α sites as previously reported. The enhancement of intrinsic activity of Co^{2+} sites with Co loading is attributed to the exchange of more distant Al pairs at high Co^{2+} loadings, leading to highly effective sites for CH_4 activation. The synthesis of Co-ZSM-5 catalysts where Co^{2+} is exclusively ion exchanged – by avoiding precipitation of inactive Co oxide particles – is critical to gain understanding of CH_4 and benzene reactions on Co^{2+} sites, as well as of the role of Co^{2+} Lewis acidity and the impact of Co^{2+} siting for the intrinsic activity of these materials.

5. Associated content

Supporting Information. S1: Synthesis of Co-ZSM-5 catalysts and acidity characterization; **S2:** Transmission electron microscopy of Co-ZSM-5 catalysts prepared by different methods; **S3:** Additional activity data of Co-ZSM-5 catalysts; **S4:** Kinetic parameters; **S5:** Supplementary information of the TPSR and TPD experiments; **S6:** Characterization of Co-ZSM-5 materials; **S7:** Analysis of location of Co exchanged sites in ZSM-5, based on spectroscopic measurements; **S8:** Supplementary references.

Author contributions

The manuscript was written through contributions of all authors. / All authors have given approval to the final version of the manuscript.

CRediT authorship contribution statement

Martina Aigner: Writing – original draft, Methodology, Investigation, Formal analysis, Data curation. **Stijn Van Daele:** Writing – review & editing, Resources, Formal analysis, Conceptualization. **Delphine Minoux:** Resources. **Nikolai Nesterenko:** Supervision. **Ruixue Zhao:** Formal analysis, Data curation. **Martin Baumgärtl:** Methodology, Formal analysis. **Rachit Khare:** Formal analysis, Data curation. **Andreas Jentys:** Resources, Formal analysis, Data curation. **Christian Schroeder:** Writing – review & editing, Visualization, Supervision, Data curation. **Maricruz Sanchez-Sanchez:** Writing – review & editing, Writing – original draft, Validation, Supervision, Project administration, Investigation, Conceptualization. **Johannes A. Lercher:** Writing – review & editing, Visualization, Supervision, Resources, Funding acquisition, Conceptualization.

Declaration of competing interest

The authors declare that they have no known competing financial interests or personal relationships that could have appeared to influence the work reported in this paper.

Data availability

Data will be made available on request.

Acknowledgment

J.A.L. acknowledges the support by the US Department of Energy (DOE), Office of Science, Office of Basic Energy Sciences (BES), Division of Chemical Sciences, Geosciences and Biosciences (Impact of catalytically active centers and their environment on rates and thermodynamic states along reaction paths, FWP 47319). The X-ray absorption spectroscopy measurements were performed at the P65 beamline of DESY (Hamburg, Germany), a member of the Helmholtz Association HGF. The authors acknowledge support from Dr. Edmund Welter and other staff from the P65 beamline.

Appendix A. Supplementary data

Supplementary data to this article can be found online at <https://doi.org/10.1016/j.jcat.2024.115686>.

References

- [1] W. Taifan, J. Baltrusaitis, CH_4 conversion to value added products: Potential, limitations and extensions of a single step heterogeneous catalysis, *Appl Catal B* 198 (2016) 525–547.
- [2] L.G. Pinaeva, A.S. Noskov, V.N. Parmon, Prospects for the direct catalytic conversion of methane into useful chemical products, *Catal. Ind.* 9 (4) (2017) 283–298.
- [3] L. Wang, L. Tao, M. Xie, G. Xu, J. Huang, Y. Xu, Dehydrogenation and aromatization of methane under non-oxidizing conditions, *Catal. Lett.* 21 (1) (1993) 35–41.
- [4] V. Abdelsayed, D. Shekhawat, M.W. Smith, Effect of Fe and Zn promoters on Mo/HZSM-5 catalyst for methane dehydroaromatization, *Fuel* 139 (2015) 401–410.
- [5] K. Sun, D.M. Ginosar, T. He, Y. Zhang, M. Fan, R. Chen, Progress in nonoxidative dehydroaromatization of methane in the last 6 years, *Ind. Eng. Chem. Res.* 57 (6) (2018) 1768–1789.
- [6] Y. Xu, M. Chen, T. Wang, B. Liu, F. Jiang, X. Liu, Probing cobalt localization on HZSM-5 for efficient methane dehydroaromatization catalysts, *J. Catal.* 387 (2020) 102–118.
- [7] K. Nakamura, K. Okumura, E. Tsuji, S. Suganuma, N. Katada, Reactivity of methane and benzene over metal/MFI zeolite analyzed with temperature-programmed reaction technique, *ChemCatChem* 12 (8) (2020) 2333–2340.

- [8] K. Nakamura, A. Okuda, K. Ohta, H. Matsubara, K. Okumura, K. Yamamoto, R. Itagaki, S. Suganuma, E. Tsuji, N. Katada, Direct methylation of benzene with methane catalyzed by Co/MFI zeolite, *ChemCatChem* 10 (17) (2018) 3806–3812.
- [9] H. Matsubara, E. Tsuji, Y. Moriwaki, K. Okumura, K. Yamamoto, K. Nakamura, S. Suganuma, N. Katada, Selective formation of active cobalt species for direct methylation of benzene with methane on MFI zeolite by co-presence of secondary elements, *Catal. Lett.* 149 (9) (2019) 2627–2635.
- [10] P. Hu, K. Nakamura, H. Matsubara, K. Iyoki, Y. Yanaba, K. Okumura, T. Okubo, N. Katada, T. Wakihara, Comparative study of direct methylation of benzene with methane on cobalt-exchanged ZSM-5 and ZSM-11 zeolites, *Appl. Catal. A* 601 (2020) 117661.
- [11] M.O. Adebajo, Green chemistry perspectives of methane conversion via oxidative methylation of aromatics over zeolite catalysts, *Green Chem.* 9 (2007) 526–539.
- [12] D.B. Lukyanov, T. Vazhnova, Selective and stable benzene alkylation with methane into toluene over PtH-MFI bifunctional catalyst, *J. Mol. Catal. A Chem.* 305 (1–2) (2009) 95–99.
- [13] H. Matsubara, K. Yamamoto, E. Tsuji, K. Okumura, K. Nakamura, S. Suganuma, N. Katada, Position and Lewis acidic property of active cobalt species on MFI zeolite for catalytic methylation of benzene with methane, *Microporous Mesoporous Mater.* 310 (2021) 110649.
- [14] J. Dědeček, D. Kaucký, B. Wichterlová, O. Gonsiorová, Co²⁺-ions as probes of Al distribution in the framework of zeolites. ZSM-5 study, *Phys. Chem. Chem. Phys.* 4 (21) (2002) 5406–5413.
- [15] A.A. Gabrienko, S.S. Arzumanov, A.V. Toktarev, I.G. Danilova, I.P. Prosvirin, V. V. Kriventsov, V.I. Zaikovskii, D. Freude, A.G. Stepanov, Different Efficiency of Zn²⁺ and ZnO species for methane activation on Zn-modified zeolite, *ACS Catal.* 7 (3) (2017) 1818–1830.
- [16] S. Grundner, W. Luo, M. Sanchez-Sanchez, J.A. Lercher, Synthesis of single-site copper catalysts for methane partial oxidation, *Chem. Commun.* 52 (12) (2016) 2553–2556.
- [17] L. Tao, I. Lee, M. Sanchez-Sanchez, Cu oxo nanoclusters for direct oxidation of methane to methanol: formation, structure and catalytic performance, *Catal. Sci. Technol.* 10 (21) (2020) 7124–7141.
- [18] A. Oda, H. Torigoe, A. Itadani, T. Ohkubo, T. Yumura, H. Kobayashi, Y. Kuroda, An important factor in CH₄ activation by Zn ion in comparison with Mg ion in MFI: The superior electron-accepting nature of Zn²⁺, *J. Phys. Chem. C* 118 (28) (2014) 15234–15241.
- [19] A.S.S. Wilson, M.S. Hill, M.F. Mahon, C. Dinioi, L. Maron, Organocalcium-mediated nucleophilic alkylation of benzene, *Science* 358 (6367) (2017) 1168–1171.
- [20] X. Zhao, D. Xiao, X. Cui, C. Chai, L. Zhao, Mechanistic insight into the organocalcium-mediated nucleophilic alkylation of benzene and further rational design, *Catal. Sci. Technol.* 10 (4) (2020) 950–958.
- [21] A. Bellmann, C. Rautenberg, U. Bentrup, A. Brückner, Determining the location of Co²⁺ in zeolites by UV-Vis diffuse reflection spectroscopy: A critical view, *Catalysts* 10 (1) (2020) 123.
- [22] A. Bellmann, H. Atia, U. Bentrup, A. Brückner, Mechanism of the selective reduction of NO_x by methane over Co-ZSM-5, *Appl. Catal. B* 230 (2018) 184–193.
- [23] L. Drozdová, R. Prins, J. Dědeček, Z. Sobalík, B. Wichterlová, Bonding of Co Ions in ZSM-5, ferrierite, and mordenite: An X-ray absorption, UV-Vis, and IR study, *J. Phys. Chem. B* 106 (9) (2002) 2240–2248.
- [24] A.B. Ene, T. Archipov, E. Roduner, Spectroscopic study of the adsorption of benzene on Cu/HZSM5 zeolites, *J. Phys. Chem. C* 114 (34) (2010) 14571–14578.
- [25] M. Baumgärtl, A. Jentys, J.A. Lercher, Influence of acid sites on xylene transport in MFI type zeolites, *J. Phys. Chem. C* 124 (7) (2020) 4134–4140.
- [26] B.C. Knott, C.T. Nimlos, D.J. Robichaud, M.R. Nimlos, S. Kim, R. Gounder, Consideration of the aluminum distribution in zeolites in theoretical and experimental catalysis research, *ACS Catal.* 8 (2) (2018) 770–784.
- [27] D.E. Perea, I. Arslan, J. Liu, Z. Ristanović, L. Kovarik, B.W. Arey, J.A. Lercher, S. R. Bare, B.M. Weckhuysen, Determining the location and nearest neighbours of aluminium in zeolites with atom probe tomography, *Nat. Commun.* 6 (1) (2015) 7589.
- [28] N. Katada, N. Ozawa, E. Tsuji, K. Kanehara, A. Otsuka, T. Sakamoto, K. Umezawa, H. Matsubara, S. Suganuma, M. Kubo, Methylation of benzene with methane induced by strong adsorption of benzene on Co ion at α -position in zeolite with moderate Al–Al distance, *Microporous Mesoporous Mater.* 364 (2024) 112855.
- [29] A. Oda, H. Torigoe, A. Itadani, T. Ohkubo, T. Yumura, H. Kobayashi, Y. Kuroda, Mechanism of CH₄ activation on a monomeric Zn²⁺-ion exchanged in MFI-type zeolite with a specific Al arrangement: similarity to the activation site for H₂, *J. Phys. Chem. C* 117 (38) (2013) 19525–19534.
- [30] L. Benco, T. Bucko, J. Hafner, H. Toulhoat, Periodic DFT calculations of the stability of Al/Si substitutions and extraframework Zn²⁺ cations in mordenite and reaction pathway for the dissociation of H₂ and CH₄, *J. Phys. Chem. B* 109 (43) (2005) 20361–20369.
- [31] D. Nozik, F.M.P. Tinga, A.T. Bell, Propane dehydrogenation and cracking over Zn/H-MFI prepared by solid-state ion exchange of ZnCl₂, *ACS Catal.* 11 (23) (2021) 14489–14506.
- [32] A. Janda, A.T. Bell, Effects of Si/Al ratio on the distribution of framework Al and on the rates of alkane monomolecular cracking and dehydrogenation in H-MFI, *J. Am. Chem. Soc.* 135 (51) (2013) 19193–19207.